Biochemistry

 Volume 35, Number 5 February 6, 1996

Accelerated Publications

Cytidine Deaminase Complexed to 3-Deazacytidine: A "Valence Buffer" in Zinc Enzyme Catalysis†

Shibin Xiang,‡ Steven A. Short,§ Richard Wolfenden,‡ and Charles W. Carter, Jr.*,‡

Department of Biochemistry and Biophysics, University of North Carolina at Chapel Hill, Chapel Hill, North Carolina 27599-7260, and Division of Experimental Therapy, Welcome Research Laboratory, Research Triangle Park, North Carolina 27709

Received October 27, 1995; Revised Manuscript Received December 6, 1995⊗

ABSTRACT: The cytidine deaminase substrate analog inhibitor 3-deazacytidine binds with its 4-amino group inserted into a site previously identified as a probable binding site for the leaving ammonia group. Binding to this site shifts the pyrimidine ring significantly further from the activated water molecule than the position it occupies in either of two complexes with compounds capable of hydrogen bonding at the 3-position of the ring [Xiang et al. (1995) *Biochemistry 34*, 4516−4523]. Difference Fourier maps between the deazacytidine, dihydrozebularine, and zebularine−hydrate inhibitor complexes suggest that the ring itself moves successively toward the activated water, leaving the amino group behind in this site as the substrate complex approaches the transition state. They also reveal systematic changes in a single zinc−sulfur bond distance. These correlate with chemical changes expected as the substrate approaches the tetrahedral transition state, in which the zinc-activated hydroxyl group develops maximal negative charge and forms a short hydrogen bond to the neighboring carboxylate group of Glu 104. Empirical bond valence relationships suggest that the Zn−S_γ132 bond functions throughout the reaction as a "valence buffer" that accommodates changing negative charge on the hydroxyl group. Similar structural features in alcohol dehydrogenase suggest that analogous mechanisms may be a general feature of catalysis by zinc enzymes.

Cytidine deaminase (CDA)[1] is one of the more efficient enzymes known (Radzicka & Wolfenden, 1995), increasing the rate of hydrolytic deamination of cytidine to uridine roughly 10^{11}-fold (Frick et al., 1987). The active site is built around a zinc ion coordinated in a tetrahedral ligand field to two cysteine thiolate ligands (Cys 129, Cys 132), a histidine (His 102), and the substrate water molecule. Of these zinc-liganding residues, substitution for Cys 132 produced the most severe effects on catalysis and protein stability (Smith et al., 1994). Catalysis also depends critically on hydrogen-bonding and proton transfer functions provided by the carboxylate side chain of Glu 104, since mutation of that residue to alanine reduced activity by 10^8-fold (Carlow et al., 1994). To understand the catalytic mechanism, we have compared X-ray crystal structures of stable intermediate states achieved using different inhibitors. We have described structures approximating the transition state complex by hydrated pyrimidin-2-one ribonucleoside inhibitors zebularine

† This work was supported by a grant from the American Cancer Society (BE-54B).

* Author to whom correspondence should be addressed: telephone, (919) 966-3263; FAX, (919) 966-2852; E-mail, carter@med.unc.edu.

‡ University of North Carolina at Chapel Hill.

§ Welcome Research Laboratory.

⊗ Abstract published in *Advance ACS Abstracts*, January 15, 1996.

[1] Abbreviations: CDA, cytidine deaminase; ADA, adenosine deaminase; DAC, 3-deazacytidine; ZEB, zebularine or pyrimidin-2-one riboside; ZEB-H_2O, zebularine 3,4-hydrate; FZEB, 5-fluorozebularine; DHZ, 3,4-dihydrozebularine; DAA, 1-deazaadenosine.

0006-2960/96/0435-1335$12.00/0

Table 1: Crystallographic Data for CDA·DAC Complex

data		refinement	
resolution limit (Å)	2.3	protein atoms	2220
no. of observations	131378	ligand atoms	16
no. of unique reflections	27432	zinc ion	1
completeness (%)	90	ordered waters	50
R_{merge} (%)	6.5	*R*-factor	0.17
		rms bond length deviation (Å)	0.008
		rms bond angle deviation (deg)	1.8

(ZEB-H_2O) and 5-fluorozebularine (FZEB-H_2O) and by 3,4-dihydrozebularine (DHZ), in which one crucial binding determinant of the transition state, the 4-OH group, is replaced by a hydrogen atom (Betts et al., 1994; Xiang et al., 1995).

A revealing observation from that comparison was a positive peak centered on the Zn−S_γ132 bond in the $\{|F_{CDA\cdot DHZ}| - |F_{CDA\cdot ZEB}|, \phi_{CDA\cdot ZEB}\}$ difference Fourier map, indicating an increased Zn−S bond distance in the ZEB-H_2O complex (Xiang et al., 1995). In addition to this alteration in the zinc coordination sphere, there was an indication of a short hydrogen bond between the 4-OH group and a neighboring carboxylate group (Glu 104) in the transition state analog complexes but not in the complex to DHZ. Differences in zinc coordination geometry have also been observed for different crystal forms of other zinc enzymes (Ecklund et al., 1986; Christianson & Lipscomb, 1989; Christianson, 1991), but their role in catalysis remains unclear.

This paper describes a complex of CDA with 3-deazacytidine (DAC), whose structure closely approximates the ground state complex with its substrate, cytidine. Comparison with the previously solved complexes reveals a progressive series of structural changes in zinc coordination that are correlated with the electronic properties of the bound ligands and appear to implicate these changes in catalysis.

EXPERIMENTAL PROCEDURES

Crystals of the CDA·DAC complex (space group $P3_121$; $a = b = 120.3$ Å, $c = 78.4$ Å, $\beta = 120°$) were grown by vapor diffusion in hanging drops initially containing 14−20% saturated ammonium sulfate (pH 6.2) 11− 16 mg/mL protein previously equilibrated with 2 mM inhibitor against 1.5 mL reservoirs of 32−45% saturated ammonium sulfate at 4 °C. X-ray data were collected at 21 °C using an RAXIS II image plate and Rigaku RU-200 rotating anode. The CDA·FZEB model with FZEB deleted was used to initiate refinements of CDA·DAC, and DAC was rebuilt into the $\{|F_o| - |F_c|, \phi_c\}$ map before further refinement.

Structure refinement was carried out in the same manner used for the CDA·ZEB (Xiang et al., 1995), CDA·FZEB-H_2O (Betts et al., 1994; Xiang et al., 1995), and CDA·DHZ (Xiang et al., 1995) complexes described previously. Stereochemical restraints on active site atoms were adjusted empirically until the refinement gave a flat $\{|F_o| - |F_c|, \phi_c\}$ difference Fourier map. Between refinements with X-PLOR (Brunger et al., 1987; Brunger, 1988) and then with TNT (Tronrud et al., 1987), the model was rebuilt from both $\{2|F_o| - |F_c|\}$ and $\{|F_o| - |F_c|\}$ maps using FRODO (Jones, 1985). A well-resolved, spherical electron density peak between that for DAC and the zinc ion was interpreted to be a zinc-bound water molecule and refined as an oxygen atom. Other water molecules were added after the overall *R*-factor to 2.3 Å resolution reached a value less than 23%, and manual rebuilding would not improve the matches between map and model. Special care was taken with active site ligands for which stereochemical parameters are uncertain. Bond length constraints involving zinc and its ligands were adjusted in reasonable ranges to satisfy the criteria that the $\{|F_o| - |F_c|\}$ map should be flat (Table 1).

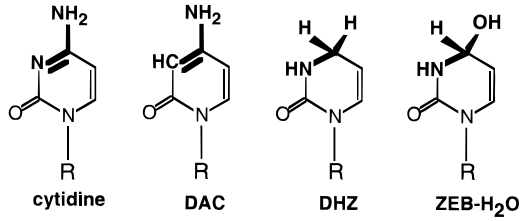

FIGURE 1: Differences between the substrate, cytidine, and the analog inhibitors used in this study. Structural differences discussed in the text are highlighted in bold face.

RESULTS

Structural differences between the inhibitors, compared to cytidine in Figure 1, reveal that each captures a different subset of recognition determinants encountered during catalysis. DAC resembles the substrate, and hence mimics early stages of the reaction close to the putative Michaelis complex, but cannot undergo hydration of the 3−4 double bond or accept a hydrogen bond to the 3-position. DHZ has several structural characteristics of the transition state analog inhibitors, including a dissociable imide proton at N3 and a tetrahedral hybridization at C4. Thus, it bears some resemblance to an activated complex. But, since the 3−4 double bond is reduced, rather than hydrated, it lacks most of the differential binding affinity of the transition state analog inhibitors. The tetrahedral transition state involving hydration of the 3−4 double bond of cytidine is represented by the covalent hydrates of ZEB and FZEB, but catalysis is arrested for these compounds because they possess a hydrogen atom at C4, in place of the normal leaving amino group.

Thus, the succession of recognition determinants proffered by this series of inhibitors suggests that these stable mimics resemble different stages of catalysis. A key feature of this progression concerns its likely effect on the protonation state of the two carboxylate oxygen atoms of Glu 104 and, by implication, on the negative charge likely to reside on the zinc-activated nucleophile. Since the 3-methylene moiety of DAC cannot hydrogen bond to $O_\epsilon1$ of Glu 104, the latter probably remains protonated. Hence, there is little tendency for the $O_\epsilon2$ atom to withdraw the proton from the zinc-bound water molecule, leaving that atom with a minimal negative charge. In the DHZ complex, the N3 proton on the pyrimidine can be shared by $O_\epsilon1$ of Glu 104 through a hydrogen bond, thereby increasing the tendency of $O_\epsilon2$ to withdraw the proton from the zinc-bound nucleophile. In the transition state analog complexes, this effect would be maximized, and the O4 atom would be expected to develop its most significant negative charge.

The crystal structure of CDA complexed with DAC (CDA·DAC) represents a new and chemically distinct structural state, complementary to those reported previously (Xiang et al., 1995). The crystals are isomorphous to those of the other complexes we have described (Betts et al., 1994).

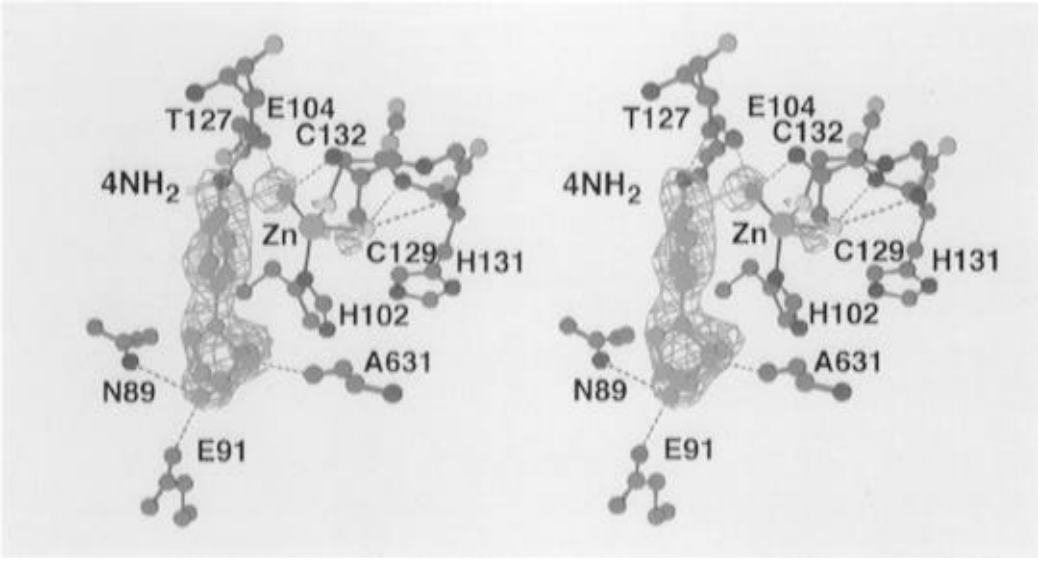

FIGURE 2: The $\{|F_o| - |F_c|, \phi_c\}$ difference density for the CDA·DAC complex, after the first cycle of X-PLOR refinement, omitting ligand atoms, and contoured at 6σ.

Nevertheless, the set of interactions between the enzyme and the DAC heterocyclic ring are distinctly different from those seen in any of the other complexes (Figures 2 and 3).

The hydrogen bond between N3 and Glu 104 observed in other complexes cannot occur with the C3 of DAC. Instead, the distance between C3 and the $O_\epsilon 1$ oxygen atom of Glu 104 is 3.0 Å, consistent with a van der Waals contact. This contact displaces the DAC ring away from Glu 104, compared to the position of DHZ (Figures 2 and 3b). The motion pivots the ring about its 2-one oxygen atom, retaining the hydrogen bond between it and the backbone amide nitrogen atom of Ala 103, leading to two new interactions.

Most striking is the location of the 4-NH_2 group of DAC, which is a progenitor of the leaving ammonia molecule. The ring displacement back from the zinc ion inserts the amino group into a pocket previously identified as a possible binding site for the leaving group (Betts et al., 1994), where it forms a hydrogen bond (2.8 Å) to the backbone carbonyl oxygen of Thr 127 (Figure 2). That C═O group is oriented, by the restricted ϕ rotation of Pro 128, in a position appropriate for hydrogen bonding to occupants of the leaving group pocket. This role of Pro 128 in binding the amino group and potentially the leaving ammonia molecule may account for the absolute conservation of this proline residue in all reported cytidine deaminases (Betts et al., 1994). Moreover, fixation of the amino group in this site suggests that it may not move much during the reaction. Rather, it seems instead that the ring itself moves away from the amino group and toward the zinc-bound water nucleophile.

As was observed for the CDA·DHZ complex (Xiang et al., 1995) and in a similar study for adenosine deaminase (ADA) complexed with an analogous inhibitor, 1-deaza-adenosine [DAA (Wilson & Quiocho, 1993)], a substrate water molecule occupies the active site (Figure 2). The improved resolution of this water molecule from the DAC ring, relative to that observed in the DHZ complex, is consistent with the refined position of DAC about 0.5 Å further from the water than is the DHZ ring. In the CDA·DHZ complex (Xiang et al., 1995), the water is indeed "trapped", pushed beneath the tetrahedral C4 hydrogen atom and a close 2.5 Å from C4, resulting in a bad van der Waals contact. The water molecule in the CDA·DAC complex is 3.0 Å from C4 and hence free of this steric strain. Moreover, it has roughly tetrahedral geometry relative to C4 (Figure 2) and appears to be ideally positioned for nucleophilic attack on the pyrimidine C4 atom.

Interactions involving the oxygen atom of the substrate water are common to the DHZ, FZEB-H_2O, and ZEB-H_2O complexes and are also retained in CDA·DAC. These include the bond to the zinc ion and hydrogen bonds to the $O_\epsilon 2$ atom of Glu 104 and the backbone amide NH group of Cys 129. The $O_\epsilon 2-O4$ distance is 2.7 Å, which is typical for a hydrogen-bonded interaction. In the two transition state analog complexes the average $O_\epsilon 2-O4$ distance, 2.45 Å, was taken to represent a short, low-barrier hydrogen bond (Xiang et al., 1995).

The significant differences between the CDA·DAC, CDA·DHZ, and CDA·Zeb-H_2O complexes are inferred from the respective $\{|F_{o,2}| - |F_{o,1}|\}$ difference Fourier maps (Figure 3). Remarkably, these three maps are nearly indistinguishable. They each exhibit features suggesting two progressive structural changes in approaching the transition state. First, matched positive and negative contours imply a steady movement of the pyrimidine ring toward the zinc and the substrate water molecule. Second, an elongated "tube" surrounding (panel c) or immediately adjacent to the $Zn-S_\gamma 132$ bond (panels a and b) implies both a progressive lengthening of that bond and a displacement of it toward the ring.

The consistent increases in the $Zn-S_\gamma 132$ bond distance shown by all three diagnostic $\{|F_{o,1}| - |F_{o,2}|\}$ difference Fourier maps represent changes in zinc coordination induced by the different active site ligands. As discussed above, these bond distance changes also correlate with the proton binding properties of Glu 104 and the substrate water molecule and hence with the likely charge development on that oxygen.

It is therefore of interest to estimate the magnitude of these effects as quantitatively as possible. Coordinate errors estimated by the statistical method of Luzzati (1952) are approximately 0.24 Å for all atoms in all structures. Estimates from the variation in polypeptide conformation among the four structures we have described are 0.15−0.17

Å for backbone atoms. These overall values overestimate errors in active site residues, which have much lower temperature factors (Betts et al., 1994). The zinc and its two thiolate ligands are probably even better determined because, being heavier than main-chain atoms, they contribute proportionately more to the scattering than do lighter protein atoms. Difference Fourier maps at 2.3 Å resolution can detect very small changes in the Zn−S_γ132 bond distance. Simulations suggest that a change of ∼0.04 Å in the Zn−S_γ132 bond would produce a peak at 3σ between the two atoms and that a correspondingly larger change is indicated by a 5σ peak.[2] Refined coordinates show a change of 0.1 Å in the Zn−S_γ132 bond distance between DAC and ZEB-H_2O complexes, consistent with the simulations.

Contour levels that give comparable features in the difference maps in Figure 3 are 5σ for the two maps involving DAC and 3.5σ for that between DHZ and ZEB-H_2O, suggesting that the major difference lies between the ground state DAC complex and either of the complexes with a protonated N3 group. This conclusion is consistent with the fact that DHZ incorporates several of the determinants for binding to the transition state analog inhibitors and with the fact that the affinity of CDA for DHZ is intermediate between those for cytidine (∼10^{-4} M) and hydrated zebularine (∼10^{-13} M). It also underscores the crucial importance of the Glu 104 O_ϵ1−N3 hydrogen bond in the approach to the transition state.

DISCUSSION

The difference Fourier maps in Figure 3 document two remarkable features of the likely CDA mechanism: the pyrimidine moves toward the activating water molecule, and the Zn−Sγ132 bond length increases as the system approaches the transition state. Movement of the pyrimidine leaves the 4-amino group behind, in the site previously identified as a likely pocket for the leaving ammonia group (Betts et al., 1994). The tetrahedral configuration of the transition state thus appears to be created by pulling the ring away from the amino group, rather than the other way round. This appears to result from a delicate calibration of the distance between the activated water molecule and the putative leaving group site created by the carbonyl oxygen of Thr 127.

Implications of the Increased Zn−S_γ132 Bond Distance for Catalysis. The progressive adjustments in the Zn−S_γ-132 bond distance from the substrate analog complex to the transition state analog complexes undoubtedly reflect the importance of this particular bond throughout the catalytic mechanism. We have already noted (Betts et al., 1994) that, at the crystallization pH of 6.2, a proton is probably transferred from the zinc-bound water molecule to the Glu 104 O_ϵ1 atom to form the catalytically active, hydroxide form of the ligand-free enzyme. This configuration may also occur in the DAC complex. Alternatively, the zinc-bound water may retain both protons in the DAC complex. In either case, since DAC cannot hydrogen bond at C3, both protons from the water are tightly associated to the Zn−water−Glu 104 system. Thus, the negative charge on the zinc-bound water is least well developed in the DAC complex, increasing monotonically, as does the Zn−S_γ132 bond length, in the progression from DAC to DHZ to the transition state analog, ZEB-H_2O. We suggest that similar reasoning holds for the catalyzed reaction, as shown schematically in Figure 4.

The increase observed in the Zn−S_γ132 bond distance implies that this bond weakens in the transition state. The simplest, electrostatic, description of such an effect would be that additional negative charge builds on the O4 atom and repels the partial negative charges on the other negatively charged ligands, S_γ132 and S_γ129, to such an extend that it overrides the expected attraction of these atoms to the Zn^{2+} ion. This net repulsive interaction must be stabilized by the enzyme for optimum catalysis to occur. As we will now describe, chemical properties of the zinc coordination sphere suggest that this stabilization occurs by changes in the Zn−S_γ132 bond distance.

A Quantitative Estimate of the "Valence-Buffer" Effect in Catalysis. A formal relationship between atomic properties and bond lengths for inorganic solids proposed by Brown (Brown & Shannon, 1973; Brown, 1992) called the "bond valence model" has proven useful in examining metalloenzymes (Thorp, 1992; Liu & Thorp, 1993). In this model, bonds to a metal are considered not to be of equal strength but rather to vary inversely with distance, according to an empirical exponential decay whose parameters reflect atomic properties such as atomic radius. The sum, $\sum_{i,j} s_{i,j}$, of these strengths or bond valences is generally observed to be close to the formal oxidation state of the metal. Zinc has a strong tendency to preserve an oxidation state of +2. The interatomic bond distance is therefore a measure of the effective charge on atoms of the coordination sphere of a metal like zinc, and changes in these distances might serve effectively as "buffers" of changes in the bond valence contributions elsewhere in the Zn coordination sphere and, more explicitly, to that of the O4−Zn bond, s_{O4-Zn}.

We infer from the effects observed in the three difference Fourier maps that the Zn−S_γ132 bond may serve as such a valence buffer during catalysis. The valence-buffering effect of changing the Zn−S_γ132 bond can be estimated quantitatively from these values using the empirical exponential relationship (Figure 5a). The average Zn−S_γ132 bond length for all four structures (2.12 Å) is short enough to fall on a steeper slope of this plot, compared with the bond lengths involving the remaining zinc ligands. The changes therefore have a large impact on bond strength. An internal check of these relationships is afforded by the bond valence sums around the zinc, which are 2.0, 2.2, 1.9, and 1.9 for the DAC, DHZ, ZEB-H_2O, and FZEB-H_2O complexes. Apparently, then, the net charge on zinc can remain nearly constant by virtue of subtle adjustments of the coordination sphere.

As noted (Xiang et al., 1995), unhindered rotation about the C_α−C_β bond of Cys 132 facilitates changing Zn−S_γ132 bond distance. Moreover, the other two protein ligands, His 102 and Cys 129, are more rigidly fixed by hydrogen bonding. In particular, S_γ129 accepts two NH--S hydrogen bonds from backbone amide nitrogen atoms in the N-cap of α-helix A (Betts et al., 1994). This arrangement is also consistent with the fact that the Zn−S_γ129 bond, 2.4 Å, is significantly longer than that for Zn−S_γ132 (Figure 5a). The

[2] We have shown that a shift of 0.04 Å from the refined Zn position produces peaks and holes at 3σ in the $\{|F_o| - |F_c|\}$ difference map. A shift of 0.06 Å is needed for S_γ132 to produce similar peaks and holes. Smaller shifts are expected to generate features of the same magnitude in $\{|F_{o,1}| - |F_{o,2}|\}$ maps, since the two sets of amplitudes share similar systematic errors, as evidenced by the *R*-factor between them (∼7%), compared to that between $|F_o|$ and $|F_c|$ (17%) (Xiang, unpublished).

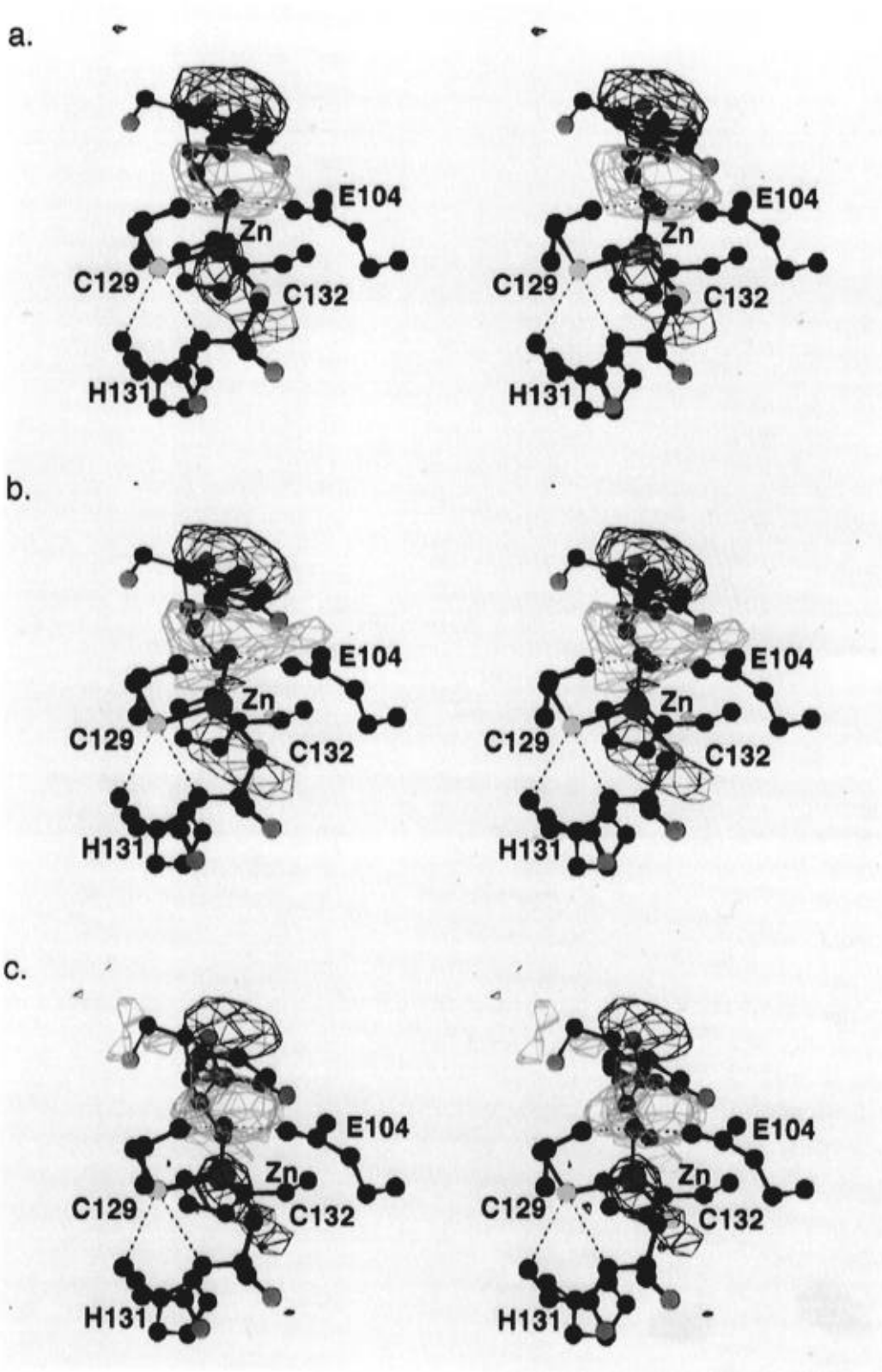

FIGURE 3: Difference Fourier maps showing active site structural differences between the CDA·DAC, CDA·DHZ, and CDA·ZEB complexes. Positive contours (purple) lie above the pyrimidine rings and surround the Zn−S_γ132 bond. Negative contours (green) lie between the pyrimidine ring and the zinc. (a) $\{|F_{CDA\cdot DAC}| - |F_{CDA\cdot FZEB}|, \phi_{CDA\cdot FZEB}\}$ map at 5σ. (b) $\{|F_{CDA\cdot DAC}| - |F_{CDA\cdot DHZ}|, \phi_{CDA\cdot DHZ}\}$ map at 5σ. (c) $\{|F_{CDA\cdot DHZ}| - |F_{CDA\cdot ZEB}|, \phi_{CDA\cdot ZEB}\}$ map at 3.5σ. The substrate water is magenta, and the illustrated inhibitors are DAC in (a) and (b) and DHZ in (c).

Zn−S_γ132 bond thus has a unique capacity to buffer changes in net negative charge in the zinc coordination sphere by moving relative to the zinc and thereby reducing or increasing its bond valence contribution. Valence buffering thus provides a mechanism for compensating developing negative charge on the substrate's 4-OH group as the reaction proceeds toward an alkoxide-like state of highest negative charge in the transition state.

Participation of the valence buffer during enzyme-catalyzed deamination could also help sustain interactions

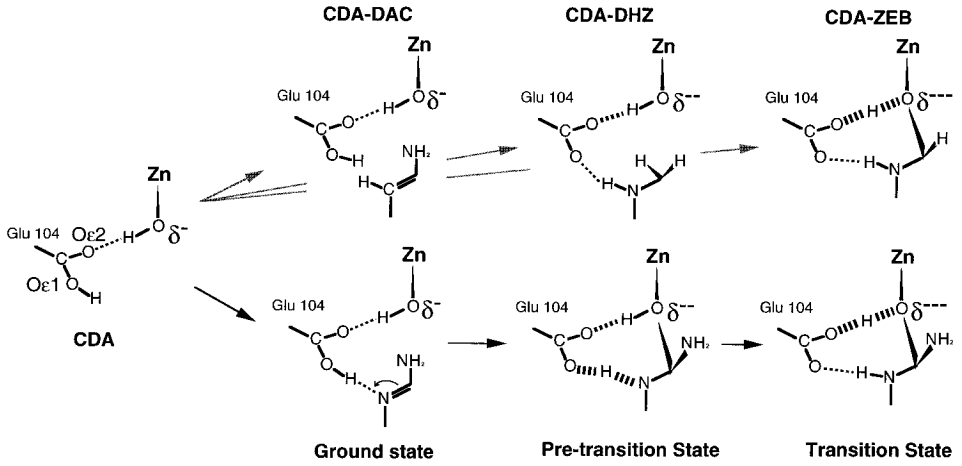

FIGURE 4: Progressive increases in the negative charge on the nucleophilic water, O4. The two ϵ oxygens of Glu 104 are labeled for clarity in the diagram for the active, ligand-free enzyme on the left. CDA crystal structures refined thus are arrayed along the top row, with proposed corresponding states of the reaction path along the bottom row. Net negative charge on the O4 atom is proposed to increase as the Glu 104 carboxylate gives up a proton to N3 (pretransition state) and then withdraws the remaining proton from O4 (transition state). These steps are indicated by the thick O--H--N hydrogen bonds in the pretransition state complex and the thick O--H--O hydrogen bonds in the transition state complex. The analogy does not imply that the CDA-DHZ complex is activated in the same way as the pre-transition state complex. The increased negative charge in that complex arises from loss of the proton from $O_\epsilon1$ of Glu 104 on binding DHZ.

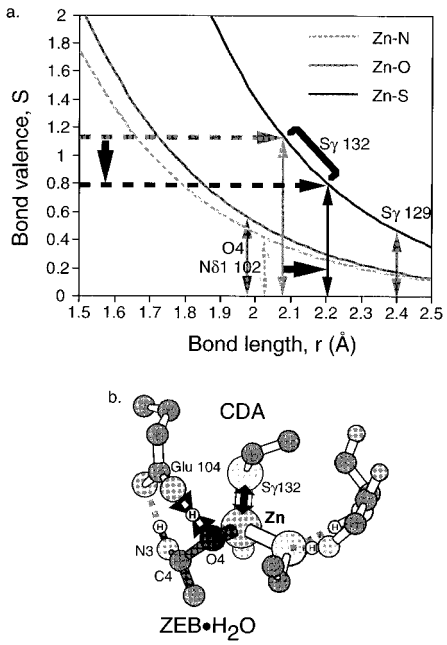

FIGURE 5: Valence-buffer mechanism. (a) Variation of bond strength vs bond length. Curves were calculated from the empirical expression for the bond valence, $S = \exp[(r_0 - r)/B]$, where r_0 and B are constants (Altermatt & Brown, 1985). In the ground state (gray dashed horizontal and solid vertical lines) the bond strength is greater; in the transition state (black dashed horizontal and solid vertical lines) it is reduced. (b) Increases in the Zn−S_γ132 bond distance are correlated with shortening of the hydrogen bond formed between Glu 104 and the 4-OH oxygen. Coupled changes implied by the arrows may facilitate formation of a low-barrier hydrogen bond between these two atoms, thereby catalyzing proton transfer to the leaving 4-NH_2 group.

between O4 and the zinc during development of negative charge on O4, thereby weakening the bond between the O4 oxygen and its proton (Figure 5b). We have proposed that this proton is already shared strongly with $O_\epsilon2$ of Glu 104 (Xiang et al., 1995); its release to that group could set the stage for subsequent transfer to the leaving ammonia group. Thus, the valence-buffering effect may be critical for lowering activation barriers associated with proton transfer steps other than formation of the tetrahedral intermediate associated with hydration of the 3−4 double bond, which is presumably rate limiting in the uncatalyzed reaction.

We expect that these effects also involve changes of the Zn−O4 distance, as well as secondary effects on other parts of the system. However, that bond lies in a region that is confounded by the structural changes involving movement of the ring. The difference Fourier maps are therefore not an unambiguous source of information about that bond, as they are for the changes in the Zn−S_γ132 bond.

Valence-Buffer Mechanisms in Other Zinc Enzymes. Valence-buffer mechanisms probably also occur in other zinc enzymes. A close replica of the two-thiolate zinc coordination has been observed in alcohol dehydrogenase (Ecklund et al., 1986; Christianson & Lipscomb, 1989; Christianson, 1991). The Zn-S distances in the CDA·DAC complex are 2.1 Å (Zn-S_γ132) and 2.4 Å (Zn−S_γ129). The Zn−S_γ132 bond serves as the valence buffer since Cys 132 is relatively more flexible than is Cys 129, the sulfur does not make hydrogen bonds to backbone NH groups, and its shorter Zn−S distance is more efficient in changing bond valence (Figure 5a). Alcohol dehydrogenase shares exactly these active site features with CDA. Its catalytic zinc ion is similarly bonded to two cysteine thiolate (Cys 46, Cys 174) and one histidine (His 67) ligand(s). Like Cys 132 in CDA, Cys 174 in alcohol dehydrogenase has a shorter Zn−S_γ bond length (2.1 Å); its S_γ atom cannot make any NH−S hydrogen bonds; and its distance from the zinc depends on the ligation state of the enzyme. On the other hand, Cys 46, whose S_γ accepts a hydrogen bond from the backbone nitrogen of Thr 48 and interacts with zinc at a longer distance of 2.4 Å, resembles Cys 129 in CDA. Thus, the Zn−S_γ174 probably plays the valence-buffer role during catalysis by alcohol dehydrogenase in a manner similar to that of the Zn−S_γ132 bond in CDA.

Most other zinc enzymes, like ADA, have no thiolate zinc ligands. Nevertheless, several zinc ligands together may play the valence-buffering role since no single Zn−N or Zn−O bond is likely to provide enough bond valence change to buffer the charge developing on the nucleophile without seriously deforming the corresponding side group configu-

ration (Figure 5a). Valence buffering is novel, in the sense that it would act throughout catalysis to reduce barriers that might arise between successive states due to stabilization of the transition state for the overall chemical reaction. Analogous mechanisms would therefore be expected for other enzymes that stabilize polar transition states. For example, they may provide the kind of catalytic improvement that differentiates enzymes from abzymes (Stewart & Benkovic, 1995). Their effects, however, would be difficult to demonstrate unequivocally by X-ray crystallography without much higher resolution data. Their appearance in our studies appears to be a fortunate coincidence of high crystal isomorphism, relatively high atomic weight of the affected atoms, and concentration of the effect on a single zinc−ligand bond.

ACKNOWLEDGMENT

We are grateful to Victor Marquez for the gift of 3-deazacytidine and to Jan Hermans, Holden Thorp, Lu Wang, and I. D. Brown for helpful discussions.

REFERENCES

Altermatt, D., & Brown, I. D. (1985) *Acta Crystallogr. B41*, 241−244.

Betts, L., Xiang, S., Short, S. A., Wolfenden, R., & Carter, C. W., Jr. (1994) *J. Mol. Biol. 235*, 635−656.

Brown, I. D. (1992) *Acta Crystallogr. B48*, 553−572.

Brown, I. D., & Shannon, R. D. (1973) *Acta Crystallogr. A29*, 266−282.

Brunger, A. T. (1988) *X-PLOR version 2.1 manual*, The Howard Hughes Medical Institute and Department of Molecular Biophysics and Biochemistry, Yale University, New Haven, CT.

Brunger, A. T., Kuriyan, J., & Karplus, M. (1987) *Science 235*, 458−460.

Carlow, D., Smith, A. A., Yang, C. C., Short, S. A., & Wolfenden, R. (1994) *Biochemistry 33*, 4220−4224.

Christianson, D. W. (1991) *Adv. Protein Chem. 42*, 281−355.

Christianson, D. W., & Lipscomb, W. N. (1989) *Acc. Chem. Res. 22*, 62−69.

Ecklund, H., Jones, T. A., & Schneider, M. (1986) in *Zinc Enzymes* (Bertini, I., Luchinat, C., Maret, W., Zeppezauer, M., Eds.) pp 377−392, Birkhauser, Boston.

Frick, L., MacNeela, J. P., & Wolfenden, R. (1987) *Biorg. Chem. 15*, 100−108.

Jones, T. A. (1985) *Meth. Enzymol. 115*, 157−171.

Liu, W., & Thorp, H. H. (1993) *Inorg. Chem. 32*, 4102−4105.

Luzzati, V. (1952) *Acta Crystallogr. 5*, 802−810.

Radzicka, A., & Wolfenden, R. (1995) *Science 267*, 90−93.

Smith, A. A., Carlow, D. C., Wolfenden, R., & Short, S. A. (1994) *Biochemistry 33*, 6468−6474.

Stewart, J. D., & Benkovic, S. J. (1995) *Nature 375*, 388−391.

Thorp, H. H. (1992) *Inorg. Chem. 31*, 1585−1588.

Tronrud, D., Ten Eyck, L. F., & Mathews, B. W. (1987) *Acta Crystallogr. A43*, 489−501.

Wilson, D. K., & Quiocho, F. A. (1993) *Biochemistry 32*, 1689−1694.

Xiang, S., Short, S. A., Wolfenden, R., & Carter, C. W., Jr. (1995) *Biochemistry 34*, 4516−4523.

BI9525583